Proton-Coupled Electron Equilibrium in Soluble and Membrane-Bound Cytochrome *c* Oxidase from *Paracoccus denitrificans*†

Ilya Belevich,‡ Anne Tuukkanen,‡ Mårten Wikström, and Michael I. Verkhovsky*

Helsinki Bioenergetics Group, Institute of Biotechnology, University of Helsinki, FIN-00014 Helsinki, Finland

Received December 1, 2005; Revised Manuscript Received January 31, 2006

ABSTRACT: The pH dependence of electron and proton re-equilibration upon CO photolysis from two-electron-reduced aa_3 oxidase was followed by time-resolved electrometry and optical spectroscopy. Optical spectroscopy on soluble *Paracoccus denitrificans* enzyme at alkaline pH revealed a slow (1 ms) component of electron re-equilibration coupled to the release of protons from the catalytic site. In the work [Brändén, M., et al. (2003) *Biochemistry 42*, 13178−13184], it was proposed that this proton is released from a water molecule in the catalytic site, located deep in the membrane dielectric. Movement of charged particles such as protons across the dielectric should create an electric potential. However, recording of the time course of the potential generation did not show any potential development in the millisecond time domain, but instead, potential generation was found with an apparent time constant of 50−100 μs. This potential was generated upon proton release from the level of the binuclear catalytic site through the K-channel, because mutation in this channel abolishes the potential generation altogether. The apparent inconsistency between results from optical spectroscopy and electrometry was solved by optical experiments on the membrane-incorporated enzyme. Reconstituting the enzyme into proteoliposomes speeds up the slow electron redistribution process by a factor of 10 and shows the same time constant as potential generation. The possible mechanism of such dramatic change in the rate of proton transfer is discussed.

Cytochrome *c* oxidase, the terminal enzyme of the respiratory chain in all eukaryotes and many bacteria, catalyses reduction of dioxygen to water. This reaction requires four electrons and four protons, which are taken into the enzyme from opposite sides of the membrane and are transferred to the active site through the membrane dielectric (*1*, *2*). In addition, cytochrome *c* oxidase uses the energy released in the reaction to pump four protons over the whole membrane (*3*). Altogether, eight charges are transferred through the membrane during one catalytic cycle. These charge-transfer processes cause generation of an electrochemical potential across the membrane. The electrons are delivered one at a time from cytochrome *c* through Cu_A and heme *a* to the binuclear heme a_3−Cu_B center, where the chemistry of oxygen reduction to water takes place. Protons required for this reaction, as well as pumped protons, are provided by two different proton conducting pathways, named the D- and K-pathways after highly conserved amino acids (D124 and K354, *Paracoccus denitrificans* numbering) (*4*).

Electron transfer and proton pumping during catalysis form a complicated overall picture of the enzyme function. It is possible to follow partially simplified reactions of electron and proton transfer using equilibrium perturbation methods. The internal electron-transfer reactions and the proton-transfer processes coupled to them in cytochrome *c* oxidase can be studied not only in the forward reaction of oxygen reduction to water, but also in a more simple experimental model, electron backflow.

Under anaerobic conditions in the presence of CO, the partially reduced enzyme forms the so-called "mixed-valence" state, where the binuclear center is reduced, but the electron donor sites (heme *a* and Cu_A) are oxidized. Under oxygen-free conditions, a molecule of CO binds to heme a_3 instead of oxygen. Binding of CO increases the apparent redox midpoint potential of heme a_3 and traps electrons at the binuclear center. However, this binding is rather weak and CO can be easily photolyzed away from the heme by a flash of light. In a backflow experiment with two-electron-reduced mixed-valence enzyme (COMV),[1] dissociation of CO from heme a_3 leads to lowering of the apparent redox midpoint potential of heme a_3 and redistribution of electrons among the redox centers (*5*−*7*). Fast electron equilibration between heme a_3 and heme *a* first occurs on the nanosecond time scale (*8*−*10*). Then, in a slower process, connected with protein relaxation (most likely upon carbon monoxide release from Cu_B), additional electron redistribution between the hemes occurs with a time constant of 2−3 μs. The next step in the cascade of electron

† This research was supported by the Academy of Finland (Project Nos. 200726 and 44895), Biocentrum Helsinki, and Sigrid Juselius Foundation.

* To whom correspondence should be addressed. Phone: +358-9-19158005. Fax: +358-9-19159920. E-mail: Michael.Verkhovsky@helsinki.fi.

‡ These authors have contributed equally to the presented work.

[1] Abbreviations: COMV, "mixed-valence" (two-electron reduced) enzyme ligated by carbon monoxide; COFR, fully reduced enzyme ligated by carbon monoxide; $\Delta\psi$, electric membrane potential; P-side, positively charged side of the membrane (intermembrane space in mitochondria or periplasmic side in bacteria); N-side, negatively charged side of the membrane (matrix space in mitochondria or cytosol in bacteria); DM, *n*-dodecyl-β-D-maltoside; NHE, normal hydrogen electrode.

10.1021/bi052458p CCC: $33.50
Published on Web 03/04/2006

re-equilibration events happens in 30−50 μs and includes further electron redistribution between heme *a*/heme a_3 and Cu_A. In the mixed-valence enzyme, the extent of electron transfer to Cu_A is negligibly small and reaches only a few percent (*11*). At high pH, the process of electron backflow also includes an additional phase of electron redistribution between the redox centers in the millisecond time range. This process is coupled to proton release to the bulk medium via the K-pathway and includes deprotonation of a water molecule to a hydroxide ion at the binuclear center (*12*, *13*).

Here, using time-resolved optical absorption spectroscopy and electrometry, we have studied the pH-dependence of the charge-transfer processes after dissociation of carbon monoxide from soluble or membrane-incorporated two-electron-reduced cytochrome *c* oxidase from *P. denitrificans*.

MATERIALS AND METHODS

Enzyme Preparation and Reconstitution into Phospholipid Vesicles. Wild-type and mutants of cytochrome *c* oxidase from *P. denitrificans* were grown, isolated, and purified as previously described (*14*) with some modifications (*15*). Reconstitution of both isolated wild-type and mutant enzymes into proteoliposomes was done using the Bio-Beads (Bio-Rad Laboratories) method as earlier described (*8*), except that the enzyme concentration during the reconstitution was increased to 6 μM.

Preparation of Mixed-Valence Enzyme for Optical Spectroscopy. All optical samples contained 0.05% dodecyl L-D-maltoside (w/v) and 100 mM bis-Tris propane (pH 7.0, 7.5, 8.0, 8.5, 9.0, 9.3, and 9.5) or CAPS (3-[cyclohexylamino]-1-propanesulfonic acid, pH 10, 10.3, 10.5, 10.6, 10.8, 10.9, and 11.0). The concentration of *P. denitrificans* wild-type cytochrome *c* oxidase was about 8 μM. The mixed-valence CO-bound complex of cytochrome *c* oxidase was made by placing the enzyme into an anaerobic optical cuvette followed by exchange of the atmosphere inside the cuvette to argon on a vacuum line. Then, 50 mM glucose, 0.9 mg/mL glucose oxidase, and 90 μg/mL catalase were added to the sample. The glucose−glucose oxidase system lowers the redox potential (E_h) of the medium, which leads to reduction of the binuclear center and binding of CO to heme a_3. To trap the enzyme in the two-electron-reduced state, 100 μM of potassium ferricyanide was added to the sample prior the experiment. Addition of anaerobic ferricyanide keeps the E_h of the medium at the level of two-electron-reduced enzyme and works as a redox buffer. Formation of CO-bound mixed-valence enzyme was done under 100% CO atmosphere and verified by optical absorption spectroscopy at 590 nm.

Time-Resolved Optical Absorption Spectroscopy Measurements. Time-resolved single-wavelength absorption measurements in the α region were made using a split-beam dual-PMT spectrophotometer build in-house with a xenon flash lamp (Zeiss BL40, length of stable impulse, 5 ms) as the probe light source. Light from the xenon lamp was passed through a monochromator and then divided into two beams by partial reflection from a glass coverslip. The transmitted beam was passed through the sample compartment before being detected by a photomultiplier tube (PMT). The reflected beam was directed straight into the second PMT omitting the sample. Both PMTs were shielded from excitation light by slits and colored by 532 nm notch filters. The signals from the PMTs were digitized by a two-channel Gage85 board controlled by software written by Dr. Nikolai Belevich. Because of limitations of the light source and the Gage digitizing board, the useful time domain of this experimental setup is from 30 ns to 5 ms. The full kinetic spectra of the backflow phases in the Soret and α regions were measured using a homemade imaging spectrograph (Triax, Jobin Yvon Ltd.)−CCD camera (Andor Technology) system. Measurements at 820 nm were carried out with a separate homemade setup. A photodiode was used to record the absorbance as functions of time at 820 nm. A laser diode (ThorLabs) was used as a probe beam. In all cases, the heme a_3−CO bond was photolyzed by a laser flash (Quantel BrilliantB, frequency doubled YAG, 532 nm, pulse energy = 50 mJ).

The Setup for Electrometric Measurements. The electrometric measuring system consists of a cell which is divided into two compartments by a phospholipid measuring membrane. Vesicles with reconstituted cytochrome *c* oxidase were attached to the measuring membrane. Ag/AgCl electrodes situated on different sides of the membrane measure the electric potential generated during the enzyme reaction. The recorded voltage is proportional to the translocation of charge inside the enzyme and perpendicular to the membrane plane.

For details of the electrometric method and sample preparation, see ref *8*. It is important to mention that proteoliposomes were fused to the measuring membrane at pH 7.5, and then the buffer was replaced with medium of the desired pH.

Preparation of the Mixed-Valence Enzyme for Electrometric Measurements. The electrometric cell was placed into a gastight box and further treated similarly to the optical sample. However, concentrations of glucose oxidase and ferricyanide were increased to 3.5 mg/mL and 5 mM, respectively. To facilitate the rate of enzyme reduction, 3 μM of hexaammine−ruthenium(III) was added to the sample before putting it into the gastight box. The pH and redox potential of the medium were determined during the measurement with corresponding electrodes attached to the system. The heme a_3−CO bond was photolyzed by a laser pulse, and the membrane potential generation by the enzyme after the dissociation of CO was followed as a function of time.

RESULTS

Electron Redistribution upon Photolysis of CO from Soluble COMV aa_3 Oxidase at Different pH. We have used time-resolved optical absorption spectroscopy to study the electron backflow process in the mixed-valence enzyme. Both single- and multiwavelength measurements were made to follow the pH dependence of the backflow phases and to characterize their kinetic difference spectra. The total extent of electron transfer between the binuclear site and the donor part (Cu_A, heme *a*) of the enzyme at different pH can be determined by measuring the CO recombination rate in the mixed-valence (COMV) and fully reduced enzymes (COFR) (Figure 1). In contrast to *Rhodobacter sphaeroides* aa_3 (*16*), the CO recombination kinetics for COFR and COMV *P. denitrificans* enzymes were monophasic and can be well-fitted by a single exponential at any pH from 7 to 11 (Figure 1A). The CO recombination rate in fully reduced enzyme

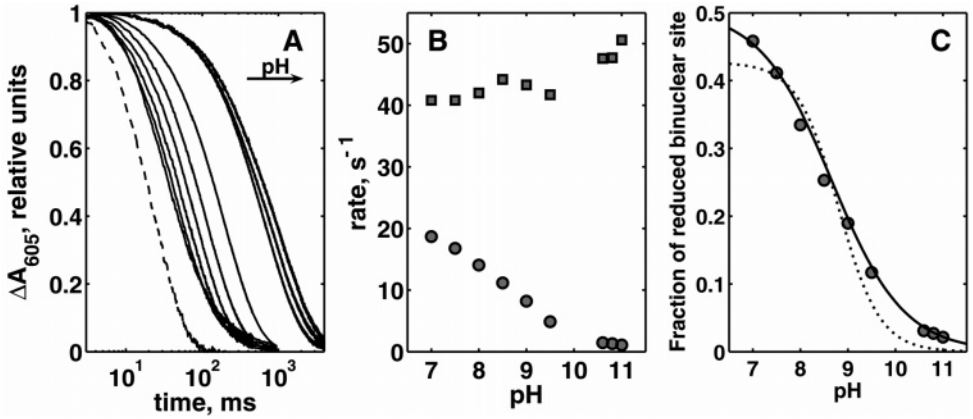

FIGURE 1: (A) Normalized absorbance changes at 605 nm corresponding to CO recombination for fully reduced enzyme (dashed line) and mixed-valence enzyme at different pH conditions (solid lines) as characterized by an arrow (pH values are 7, 7.5, 8, 8.5, 9, 9.5, 10.6, 10.8, and 11). (B) The pH dependence of the CO-recombination rate in mixed-valence (circles) and fully reduced enzyme (squares). (C) The calculated (eq 1) pH dependence of the fraction of the fully reduced binuclear center. The solid curve is a fit of the data with a Henderson−Hasselbalch one-proton titration curve (pK_a = 8.66, Hill coefficient 0.6, maximal extent 0.505). The dotted curve is a best fit with a standard one-proton titration curve (pK_a = 8.8, Hill coefficient is 1.0). Conditions: see Materials and Methods; number of averages is 25.

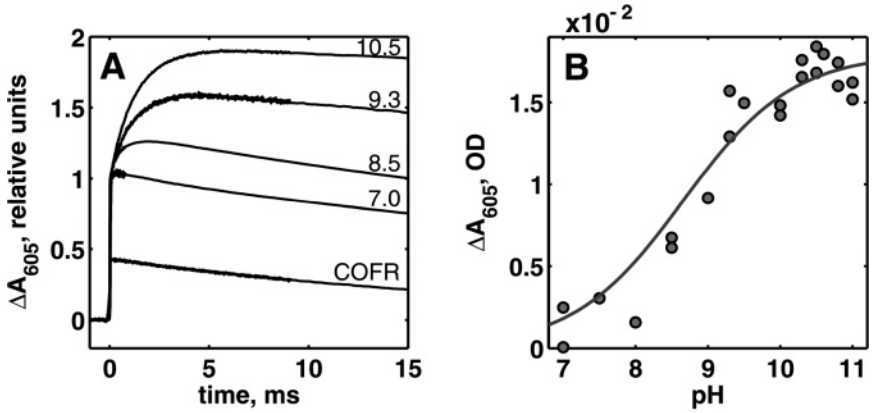

FIGURE 2: (A) Absorbance changes at 605 nm during photodissociation of CO from mixed-valence and fully reduced enzyme at specified by pH values. (B) The amplitude of the slow kinetic phase at 605 nm as a function of pH. The solid curve is a fit of the data by one-proton titration curve (pK_a = 8.66, Hill coefficient 0.6). Conditions: see Materials and Methods; number of averages is 25.

did not show any pH dependence and was about 44 s^{-1}, whereas the rate in the mixed-valence enzyme slowed from 20 s^{-1} at pH 7 to 1 s^{-1} at pH 11 (Figure 1B). The pH independence of the CO-recombination rate in fully reduced enzyme indicates that CO recombination as such does not involve protonation events. The decrease in the rate of CO recombination with pH in the mixed-valence enzyme can be explained by a decrease of the occupancy of fully reduced binuclear site after photolysis due to electron transfer from heme a_3 to heme *a*. Hence, the rate of CO recombination in the mixed-valence enzyme can be described by the following equation:

$$k_{rec}(\mathrm{pH}) = k_0[a_3^{red}(\mathrm{pH})] \quad (1)$$

where k_{rec} is the apparent rate constant of CO recombination measured at a particular pH; k_0 is the CO-recombination rate constant in fully reduced enzyme; and [a_3^{red}] is the fraction of fully reduced binuclear center, which can be approximated by the amount of reduced heme a_3 defined by the equilibrium constant of electron transfer between hemes *a* and a_3 (Figure 1C). The fraction of the fully reduced binuclear center varied from about 50% at pH 7 to almost 0 at pH 11. This indicates a total extent of electron transfer of about 100% to heme *a* at pH 11.

The kinetic traces of absorbance changes at 605 nm upon CO photolysis from COMV and COFR enzyme are shown in Figure 2A. The initial fast increase in absorbance in COMV is due to CO dissociation from heme a_3 and electron equilibration between heme a_3 and heme *a* with time constants of 1.2 ns (*8*, *9*) and about 3 μs (*6*−*9*) (see also Figure 8, inset). The increase of pH induces the growth of the slow phase of absorbance change seen on a millisecond time scale with a time constant of about 1.1 ms. The pH dependence of the amplitude of the slow electron transfer phase is presented in Figure 2B. This kinetic phase appears only at high pH values, and its amplitude increases with increasing pH. In the COFR sample, all redox centers are reduced and the initial fast phase seen in the Figure 2A corresponds to optical changes due to CO dissociation only.

To assign the microsecond and millisecond phases of absorbance changes following dissociation of CO from mixed-valence enzyme (at pH 9.5), we recorded the surface of optical changes in the wavelength range between 350 and 700 nm with a frequency of 1 spectrum/μs. Figure 3A presents the surface of absorbance changes as a function of

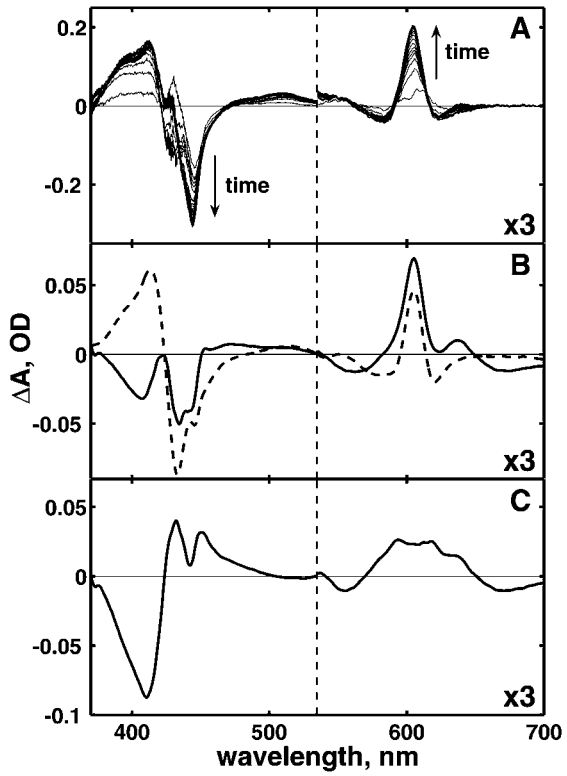

FIGURE 3: (A) Absorbance-time-wavelength surface of optical changes after CO dissociation from mixed-valence enzyme at pH 9.5. The direction of signal development in time is indicated by arrows. (B) Kinetic difference spectra of the 3 μs phase (dashed line) and the millisecond phase (solid line). (C) The difference spectrum between the two kinetic spectra in panel B. Conditions: 12 μM cytochrome *c* oxidase, 0.05% DM, 100 mM CAPS (pH 10.2), and 100% CO; number of averages is 75.

time in this wavelength range. The recorded three-dimensional absorbance-time-wavelength surface was decomposed into kinetic spectral components according to the following equation:

$$\Delta A_\lambda = \sum_{i=1}^{2} \epsilon_\lambda{}^i e^{-k_i t} + C_0 \qquad (2)$$

where ΔA_λ is the absorbance change at a particular wavelength, $\epsilon^i{}_\lambda$ is the extinction (including concentration factor) of the *i*th component at that wavelength, k_i is the rate constant of the *i*th component, *t* is time, and C_0 is the constant term characterizing the final spectrum of the product of the reaction.

Figure 3B shows the result of such decomposition. The 3 μs phase, shown as a dashed line, corresponds to the difference in the spectra of hemes *a* and a_3 and reflects electron transfer from the latter to the former. The kinetic difference spectrum of the millisecond phase, shown as a solid line, has features similar to the 3 μs electron transfer phase, but with some differences. The millisecond phase has been previously assigned to electron transfer from heme a_3 to heme *a* in a process which is coupled to proton release via the K-pathway to the bulk solution (*13*, *17*). Figure 3C presents the difference between the spectra of the 3 μs and millisecond phases. This difference spectrum resembles the spectrum of cyanide binding to ferric heme a_3, including a change from high to low spin. Brändén and co-workers (*13*) attributed the additional features in the kinetic spectrum seen in the millisecond phase to binding of a hydroxide ligand to ferric heme a_3, and our finding supports this conclusion. A shift of the typical charge-transfer band of oxidized enzyme from 660 to 635 nm is noteworthy here, as it may be a specific signature of a state of the binuclear center where Cu_B is reduced and ferric heme a_3 is ligated by hydroxide.

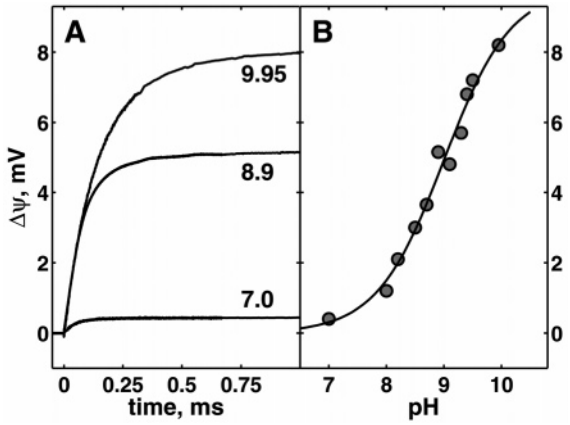

FIGURE 4: (A) The generation of membrane potential during CO photolysis from the COMV state of the enzyme at specified pH values. (B) The pH dependence of the amplitude of the electrometric response fitted with a one-proton titration curve ($pK_a = 9.0$, Hill coefficient 0.75, $A_{max} = 9.84$ mV); see details in the text. Conditions: see Materials and Methods; number of averages is 5.

Proton movement from the binuclear site located deep in the dielectric of the membrane via the K-pathway out in the medium should create an electric potential ($\Delta\psi$) with a polarity opposite to that created during enzyme turnover. To check this assignment of the millisecond phase, we studied the backflow reaction from the COMV state of the enzyme in phospholipid vesicles by an electrometric approach. Typical electrometric responses for the electron backflow reaction measured at different pH values are shown in Figure 4A. As shown before with the bovine enzyme, there is almost no $\Delta\psi$ generation in the backflow reaction at the COMV at neutral pH (*11*), and a similar picture is indeed seen for the enzyme from *P. denitrificans*. At neutral pH, the amplitude of the electrometric response is very small, reaching only about 0.25 mV. But with increasing pH, the amplitude of $\Delta\psi$ after CO photodissociation from the COMV state starts to develop and reaches 8.2 mV at pH 10. The sign of this $\Delta\psi$ generation is opposite to the $\Delta\psi$ development in the forward reaction of reduced enzyme with oxygen, indicating either electron transfer from the N- toward the P-side of the membrane, proton transfer in the opposite direction, or both.

Surprisingly, and in contrast with the optical results, the electrometric response develops in microseconds and has no detectable component in the millisecond time domain. The response can be fitted as a one-exponential process with a pH-dependent rate. At pH range from 7 to 8.5, the rate of $\Delta\psi$ generation is pH-independent ($k \sim 18\,000$ s^{-1}), but upon further movement toward the alkaline region, the rate starts to decrease and reaches 4000 s^{-1} at pH 10.5 (Figure 5).

The time constant of the electrogenic phase (50 μs in the pH range 7−8.5) is very close to the rate of electron transfer from the two hemes to the Cu_A center, and such a reaction should be electrogenic. In previous work (*11*), we showed that at neutral pH this reaction is negligible in the two-electron-reduced enzyme and can be clearly seen only in the

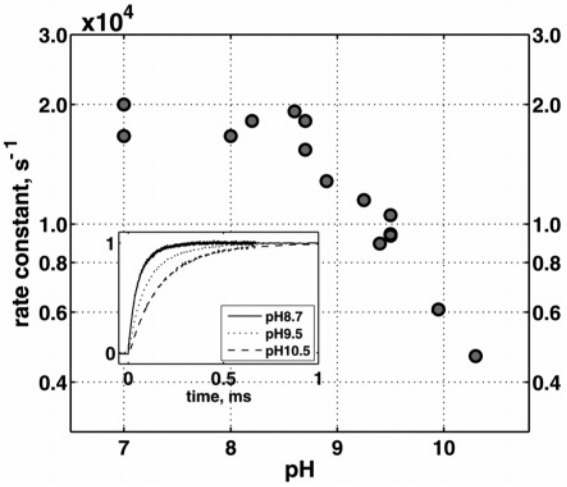

FIGURE 5: The rate of potential generation after CO photolysis from the COMV enzyme. Inset: normalized to the total amplitude traces of the electrometrical response at specified pH values. Conditions: see Materials and Methods; number of averages is 5.

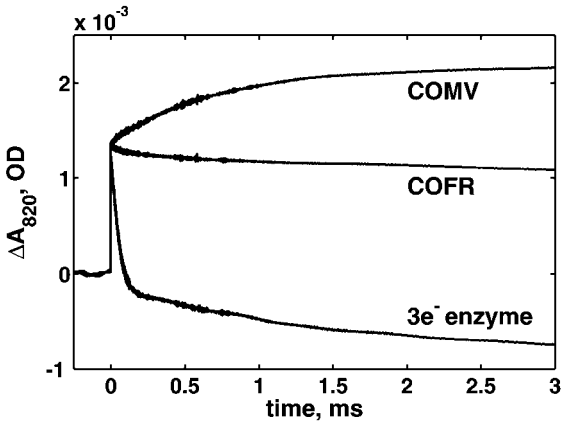

FIGURE 6: Absorbance changes at 820 nm corresponding to CO dissociation from mixed-valence, three-electron-reduced, and fully reduced enzymes at pH 9.5. The zero time is the moment of the laser flash. Conditions: see Materials and Methods; number of averages is 50.

three-electron-reduced state. To check the possibility that electron transfer to Cu_A in the COMV might start to appear at alkaline pH, we measured the redox changes of Cu_A directly by optical spectroscopy.

Time-resolved optical absorption measurements were done at alkaline pH at 820 nm, where Cu_A has a major contribution (Figure 6). First, a fast increase in the absorbance due to photolysis of CO was seen in all cases. In the mixed-valence $2e^-$ enzyme, the CO dissociation phase was followed by an increase in absorbance with a time constant of about 1.5 ms. This phase is very similar to the one detected in the experiment at 605 nm (Figure 2) and is most likely caused by electron transfer from heme a_3 to heme a. Its direction is opposite to the one expected from reduction of Cu_A. However, no fast ~50 μs decrease in absorbance corresponding to such reduction was observed. In the fully reduced enzyme, the increase of absorbance due to CO dissociation is followed by a slow CO recombination phase only, because all redox centers are reduced and no electron transfer takes place. At the $3e^-$ reduced level, a decrease in absorbance begins to appear after the initial phase, with a rate constant of about 50 μs, and this phase can be assigned to electron

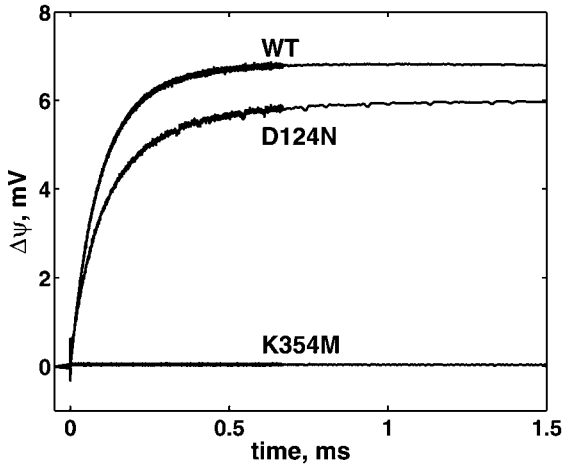

FIGURE 7: Potential generation during the electron backflow reaction in the COMV state at pH 9.5 for wild-type (WT) and proton channel mutants: K354M and D124N. Conditions: see Materials and Methods; number of averages is 5.

backflow from the hemes to Cu_A. This 50 μs component corresponds to ~10% of Cu_A reduction. The absence of such phase in the mixed-valence enzyme confirms the finding that the extent of backflow to Cu_A is very low at that redox level, even at alkaline pH. Hence, electron transfer to the Cu_A site cannot explain the electrometric response in the mixed-valence enzyme. The two heme centers and Cu_B are located at about the same depth within the membrane dielectric, so electron transfer between them cannot produce an electric potential either. Therefore, the only remaining possibility to explain the 50−100 μs phase of potential generation is that it derives from electron-coupled proton transfer from the P- toward the N-side of the membrane.

Additional support for this conclusion comes from experiments with mutant enzymes. We checked $\Delta\psi$ generation in the backflow reaction at alkaline pH in two mutants, where either the D- or the K-channel of proton transfer was blocked. The results show a clear difference between these two mutant enzymes (Figure 7). $\Delta\psi$ generation in the D124N mutant (with the block in the D-channel) is very similar to that of the wild-type enzyme. It has about the same maximal amplitude and the same rate of potential generation in alkaline conditions. In contrast, in the K354M mutant (with block of the K-channel), CO photolysis from the $2e^-$ reduced enzyme is not coupled to any charge translocation across the membrane. This agrees with previous time-resolved optical absorbance measurements on the K-channel mutant in *R. sphaeroides* where the millisecond electron-transfer phase was also reported to be absent (*18*). A redox titration of the backflow reaction in the K354M mutant from the two- to the four-electron-reduced state shows no electrogenic phase at E_h = 440−280 mV versus NHE, but in the range of redox potentials lower than 280 mV (appearance of $3e^-$ state), $\Delta\psi$ starts to develop with rate constant of 24 000 s^{-1} (not shown), corresponding to electron transfer from heme a to Cu_A, similar to the case in the wild-type enzyme at the same potentials at neutral pH. This result shows that the electron backflow reaction is present in the K354M mutant enzyme, but that it is not linked to proton transfer. We therefore conclude that the backflow electron transfer reaction in the alkaline COMV is coupled to proton transfer through the K-channel. We thus arrive at the apparently contradictory

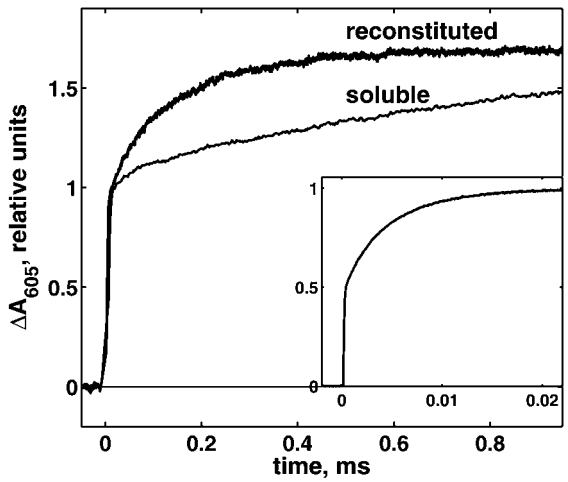

FIGURE 8: Comparison of absorbance changes at 605 nm after CO dissociation from reconstituted and soluble mixed-valence cytochrome *c* oxidase at pH 9.5. Inset: early part of the optical response at 605 nm in soluble mixed-valence enzyme. The response consists of absorbance changes due to CO photolysis and electron transfer between the hemes with time constants of 1.2 ns and 3 μs. Conditions: see Materials and Methods; number of averages is 55 for reconstituted and 25 for soluble enzyme.

conclusion that proton release via the K-pathway, coupled to electron re-equilibration, happens with a time constant of 50−100 μs, whereas electron re-equilibration itself happens at 1 ms, which is also the time constant at which protons have been seen to be ejected from the enzyme (*13*). The main difference between the two types of measurement is the enzyme surroundings. The electron-transfer reaction (and proton release) was measured with detergent-solubilized enzyme (*13*), whereas the electric potential measurements were performed with the enzyme reconstituted into phospholipid vesicles. To check the possibility that the enzyme surroundings might cause such a dramatic effect on the rate of proton release and electron re-equilibration, we measured the electron backflow reaction by optical spectroscopy in enzyme incorporated in phospholipid vesicles.

Figure 8 presents kinetic traces at 605 nm with reconstituted and soluble enzyme. The rate of the second electron transfer backflow phase is significantly slower in the soluble enzyme than in the reconstituted enzyme at the same pH. Corresponding rates for soluble and reconstituted enzymes were 1.1 ms and about 150 μs (at pH 9.5). This finding explains the fact that the rate of proton release in reconstituted enzyme, as measured electrometrically, is significantly higher than the rate of electron transfer coupled to that proton release in soluble enzyme. The difference in rates apparently reflects the difference in the equilibrium properties of the K-pathway in soluble and reconstituted enzyme.

DISCUSSION

Upon photolysis of CO at alkaline pH from the soluble enzyme in the mixed-valence state, fast (nanosecond to microsecond) electron transfer from heme a_3 to heme *a* is followed by proton release from the enzyme through the K-pathway to the bulk medium, and concurrent further electron backflow in the millisecond time regime. At the same time, a water molecule at the active site deprotonates to form a hydroxide anion, which binds to ferric heme a_3. Brändén and co-workers (*13*) compared the kinetic difference spectra of the 3 μs phase and the millisecond phase upon CO-dissociation from the mixed-valence *R. sphaeroides* enzyme and concluded that the millisecond phase is not connected to electron transfer between the hemes. They also claimed that the extent of electron backflow is 100% already during the 3 μs phase at pH 7. We observed a pH dependence of the total extent of electron transfer in the CO-recombination experiments with the *P. denitrificans* enzyme. The extent of the total electron transfer increases from 50% at pH 7 to 100% at pH 11. Our analysis of the kinetic difference spectra of the phases supports the conclusion that the absorbance changes in the millisecond phase are connected to pH-dependent electron transfer, whereas the extent of the nanosecond and 3 μs electron-transfer phases are pH-independent. We used the Henderson−Hasselbalch one-proton titration curve to model the pH dependence of the fraction of reduced heme a_3 after CO-photolysis (the solid curve in Figure 1C). The fit results in a pK_a value of 8.66 and a Hill coefficient of 0.6 with the extent of fully reduced binuclear site after the fast phase being 0.505. If the pH dependence of the extent of electron transfer were assigned solely to the millisecond time scale electron transfer, the value of the inflection point would reflect the pK_a of the group donating the proton, that is, the water molecule near heme a_3. The dotted curve in Figure 1C presents the best fit to a standard Henderson−Hasselbalch one-proton titration curve. The fit with a Hill coefficient of unity produced a pK_a value of 8.8. However, the quality of this fit is much worse than in the case of a nonunity Hill coefficient. A Hill coefficient less than unity indicates negative cooperativity with several other titratable groups. It is important to stress that such groups should be located far from the titratable water molecule in the binuclear site, rather than being groupd near that site, because in the latter case we would explicitly expect a split of the titration curve reflecting direct interactions instead of a decrease in the Hill coefficient. The same conclusion can be made, independently, from the absence of any pH dependence of the amplitude of the nanosecond and 3 μs phases of electron transfer. After these phases, the enzyme reaches a state where the electrons are equilibrated in a ratio of about 50:50 between the two heme groups. This state is expected to be extremely sensitive to the charge surroundings. If anyone of the closely located groups, such as the heme propionates, tyrosine-288, or histidines, are capable of changing their protonation state in the tested pH range, the changes in charge should significantly influence the equilibrium constant of electron transfer between two hemes and alter the amplitude of the fast electron-transfer processes. However, in the experiments, we do not see any changes in the amplitude of the nanosecond or 3 μs phases, and we therefore conclude that none of the groups (except a water molecule at the catalytic site) relevant to the pump mechanism change their protonation state in the pH range from 7 to 10 in the mixed-valence enzyme. The pH dependence of the amplitude of the millisecond absorbance changes at 605 nm presented in Figure 2B was also well-fitted with the same parameters (pK_a and Hill coefficient) as the data in Figure 1C. On the basis of these two independent approaches, we conclude that the soluble enzyme has a pK_a value of 8.7 attributable to the water molecule bound to ferric heme a_3.

We observed an electrogenic phase of membrane potential generation with a time constant of about 150 μs (at alkaline pH) after dissociation of CO from the mixed-valence enzyme.

No further electrogenic phase was present in the time scale of milliseconds. The pH dependence of the amplitude of this phase implies a connection to proton transfer. Time-resolved measurements of absorbance changes at 820 nm showed no electron transfer to Cu_A (Figure 6). This verifies that the observed electrometric phase is connected to proton release to the N-side of the membrane rather than electron transfer to Cu_A.

In the K354M mutant in the mixed-valence state, this phase of membrane potential generation was absent, which suggests that proton release occurs via the K-pathway. The redox titration of the electrometric response in the K354M mutant mixed-valence enzyme showed no $\Delta\psi$ generation; at the same time, electric potential in the three-electron-reduced state due to electron transfer to Cu_A was observed. This finding shows that the mutant enzyme is capable of performing the electron backflow reaction, but this reaction is not coupled to proton release. On the other hand, the D-pathway mutation (D124N) had almost no effect on the proton release in the mixed-valence state. These results are consistent with the findings that the uptake of the first and second proton during the catalytic cycle starting from oxidized enzyme takes place through the K-pathway (*18*, *19*).

When the electrometric measurements are used, it is possible to estimate the distance of proton translocation in the backflow reaction. The $\Delta\psi$ generation in the reaction of the fully reduced cytochrome *c* oxidase with oxygen at neutral pH obtained on the same sample gives an amplitude of around 105 mV (data not shown). In this reaction, the enzyme goes from the R state via A, P, and F intermediates to the fully oxidized state, and this process corresponds to an overall movement of 3.7 charges across the phospholipid membrane (*20*). Therefore, overall movement of one charge across the membrane would correspond to 28.4 mV. Taking the thickness of the membrane as 30 Å and the maximum $\Delta\psi$ of the backflow process from the fit of the experimental data as 9.84 mV, it is possible to estimate the distance of proton translocation coupled to the slow phase of electron backflow. The maximal amplitude of the slow phase corresponds to the translocation of 0.505 electrons from the binuclear site to the heme *a*. Thus, the distance of a proton translocation can be estimated as (9.84 mV × 30 Å/28.4 mV × 0.505) = 20.6 Å per charge equivalent. This value (2/3 of the membrane depth from the N-side) is in very good agreement with our previous estimate of the binuclear site location at 1/3 of the membrane dielectric from the P-side (*20*).

The slow phase of backflow observed in soluble enzyme at high pH indicates electron transfer from heme a_3 to heme *a* in the millisecond time range. However, the corresponding proton release in the reconstituted enzyme is much faster and occurs on the microsecond time scale. This indicates that the interactions of the protonatable groups involved in proton translocation through the K-pathway with other charged groups differ in the soluble and reconstituted enzymes. There are at least two possible explanations of how enzyme reconstitution might affect the rate of proton transfer through the K-pathway. Either incorporation of the enzyme into vesicles significantly changes the conductivity of the K-pathway or the large negatively charged surface of the membrane may serve as a proton acceptor pool increasing the rate of proton release.

REFERENCES

1. Brzezinski, P. (2004) Redox-driven membrane-bound proton pumps, *Trends Biochem. Sci. 29*, 380−387.
2. Rich, P. R. (2003) The molecular machinery of Keilin's respiratory chain, *Biochem. Soc. Trans. 31*, 1095−1105.
3. Wikström, M. K. (1977) Proton pump coupled to cytochrome *c* oxidase in mitochondria, *Nature 266*, 271−273.
4. Vygodina, T. V., Pecoraro, C., Mitchell, D., Gennis, R., and Konstantinov, A. A. (1998) The mechanism of inhibition of electron transfer by amino acid replacement K362M in a proton channel of *Rhodobacter sphaeroides* cytochrome *c* oxidase, *Biochemistry 37*, 3053−3061.
5. Boelens, R., and Wever, R. (1979) Electron-transfer processes in carboxy-cytochrome *c* oxidase after photodissociation of cytochrome a_3^{2+}−CO, *Biochim. Biophys. Acta 547*, 296−310.
6. Oliveberg, M., and Malmström, B. G. (1991) Internal electron transfer in cytochrome *c* oxidase: evidence for a rapid equilibrium between cytochrome *a* and the bimetallic site, *Biochemistry 30*, 7053−7057.
7. Verkhovsky, M. I., Morgan, J. E., and Wikström, M. (1992) Intramolecular electron transfer in cytochrome *c* oxidase: a cascade of equilibria, *Biochemistry 31*, 11860−11863.
8. Verkhovsky, M. I., Tuukkanen, A., Backgren, C., Puustinen, A., and Wikström, M. (2001) Charge translocation coupled to electron injection into oxidized cytochrome *c* oxidase from *Paracoccus denitrificans*, *Biochemistry 40*, 7077−7083.
9. Pilet, E., Jasaitis, A., Liebl, U., and Vos, M. H. (2004) Electron transfer between hemes in mammalian cytochrome *c* oxidase, *Proc. Natl. Acad. Sci. U.S.A. 101*, 16198−16203.
10. Jasaitis, A., Rappaport, F., Pilet, E., Liebl, U., and Vos, M. H. (2005) Activationless electron transfer through the hydrophobic core of cytochrome *c* oxidase, *Proc. Natl. Acad. Sci. U.S.A. 102*, 10882−10886.
11. Jasaitis, A., Verkhovsky, M. I., Morgan, J. E., Verkhovskaya, M. L., and Wikström, M. (1999) Assignment and charge translocation stoichiometries of the electrogenic phases in the reaction of cytochrome *c* with dioxygen, *Biochemistry 38*, 2697−2706.
12. Hallén, S., Brzezinski, P., and Malmström, B. G. (1994) Internal electron transfer in cytochrome *c* oxidase is coupled to the protonation of a group close to the bimetallic site, *Biochemistry 33*, 1467−1472.
13. Brändén, M., Namslauer, A., Hansson, O., Aasa, R., and Brzezinski, P. (2003) Water-hydroxide exchange reactions at the catalytic site of heme-copper oxidases, *Biochemistry 42*, 13178−13184.
14. Riistama, S., Laakkonen, L., Wikström, M., Verkhovsky, M. I., and Puustinen, A. (1999) The calcium binding site in cytochrome aa_3 from *Paracoccus denitrificans*, *Biochemistry 38*, 10670−10677.
15. Ribacka, C., Verkhovsky, M. I., Belevich, I., Bloch, D. A., Puustinen, A., and Wikström, M. (2005) An elementary reaction step of the proton pump is revealed by mutation of tryptophan-164 to phenylalanine in cytochrome *c* oxidase from *Paracoccus denitrificans*, *Biochemistry 44*, 16502−16512.
16. Sigurdson, H., Brändén, M., Namslauer, A., and Brzezinski, P. (2002) Ligand binding reveals protonation events at the active site of cytochrome *c* oxidase; is the K-pathway used for the transfer of H(+) or OH(−)? *J. Inorg. Biochem. 88*, 335−342.
17. Hallén, S., and Brzezinski, P. (1994) Light-induced structural changes in cytochrome *c* oxidase: implication for the mechanism of electron and proton gating, *Biochim. Biophys. Acta 1184*, 207−218.
18. Ädelroth, P., Gennis, R. B., and Brzezinski, P. (1998) Role of the pathway through K(I-362) in proton transfer in cytochrome *c* oxidase from *R. sphaeroides*, *Biochemistry 37*, 2470−2476.
19. Wikström, M., Jasaitis, A., Backgren, C., Puustinen, A., and Verkhovsky, M. I. (2000) The role of the D- and K-pathways of proton transfer in the function of the haem-copper oxidases, *Biochim. Biophys. Acta* 1459, 514−520.
20. Verkhovsky, M. I., Jasaitis, A., Verkhovskaya, M. L., Morgan, L., and Wikström, M. (1999) Proton translocation by cytochrome *c* oxidase, *Nature 400*, 480−483.

BI052458P